JAFIB
Original Research
Journal of Atrial Fibrillation

www. jafib.com

Computational Flow Dynamic Analysis of Right and Left Atria in Patent Foramen Ovale: Potential Links with Atrial Fibrillation

Gianluca Rigatelli[1], Marco Zuin[2], Alan Fong[3]

[1]*Section of Cardiovascular Diagnosis and Endoluminal Interventions, Rovigo General Hospital, Rovigo, Italy.*
[2]*Department of Cardiology, Rovigo General Hospital, Rovigo, Italy and Section of Internal and Cardiopulmonary Medicine, Department of Medical Science, University of Ferrara, Ferrara, Italy.*
[3]*Department of Cardiology, Clinical Research Center, Sarawak General Hospital, Sarawak, Malaysia.*

Abstract

Background: An impairment of the left atrial function similar to that usually observed in atrial fibrillation (AF) has been observed also in patients with patent foramen ovale (PFO) and permanent right-to-left shunting (RLS)

Methods: We reconstructed the geometrical model of right atrium (RA), PFO, left atrium (LA) and left atrial appendage (LAA) of 65 patients with mild (36 patients mean age 45.5±6.8 years, 24 females) or permanent (29 patients, mean age 45.1±5.3 years, 21 females) RLS using anatomical data obtained by transoesophageal echocardiography (TEE) and cardiac MRI, performed as a part of our institutional screening protocol for paradoxical embolism. Using computational fluid dynamic analysis (CFD) we assessed the vorticity magnitude in both the LA and LAA to analyse a possible rheological relationship between PFO and AF.

Results: The anatomical models, in terms of dimensions, were comparable among the patients with mild and permanent RLS. A higher vorticity magnitude was observed in the mild shunt both in the LA (101.12±21.3 vs 88.3±22.6, p=0.02) and LAA (62±14.4 vs 32.4±12.3, p<0.01) when compared to the permanent R-L shunting.

Conclusion: The lower vorticity magnitude across the LA and LAA in patients with permanent RLS suggests a possible higher stagnation of the blood in these anatomical sites, similarly as previously observed in patients with AF.

Introduction

An impairment of the left atrial function similar to that usually observed in atrial fibrillation (AF) has been observed in patients with patent foramen ovale (PFO) and permanent right-to-left shunting (RLS)[1]. Computational fluid dynamic (CFD) analysis suggested that in left atrial appendage(LAA)vortices generated in the chamber remain high strength and with longer durations in patients with AF, inducing ineffective emptying of the blood into the atriumand appendage, which then lead to blood stagnation and subsequent thrombus formation[2]. Moreover, atrial wall movements inducedby high-frequency fibrillation had a large impact on the stagnation of blood flow. The relative residence time (RRT),which is an indicator of stagnation of blood flow, increases in the upper part of the LAA during AF.Atrial vulnerability and atrial abnormalities such as patent foramen ovale(PFO) and atrial septal aneurysm(ASA) have been suggested to be associated in patients with cryptogenetic stroke[3]. Finally, an anti-arrhythmic effect has been postulated for transcatheter PFO closure[4], reinforcing the hypothesis that AF and PFO might be linked. Aim of this study is to differentiateby means of CFD the fluid dynamic profile, especially the vorticity magnitude, in the LA and LAA of patients with mild/no RLS and permanent RLS.

Key Words

Computed Flow Dynamic, Atrial Fibrillation, Patent Foramen Ovale, Physiology.

Corresponding Author
Gianluca Rigatelli, Cardiovascular Diagnosis and Endoluminal Interventions Santa Maria della Misericordia Hospital, Viale Tre Martiri 140, 45100 Rovigo, Italy

Material and Methods

Overview

The geometrical model of the right atrium (RA), left atrium (LA), left atrial appendage (LAA) and PFO has been constructed reviewing the imaging data of 65normotensive otherwise healthy patients with mild (36 patients mean age 45.5±6.8 years, 24 females), or permanent RLS (29 patients, mean age 45.1±5.3 years, 21 females) evaluated through TEE and cardiac MRI, as part of our institutional screening protocol for paradoxical embolism. Patients with any grade of atrial septal aneurysm > 2 following Olivares-Reyes et al[5] have been excluded from the analysis to maintain the model homogeneous.

According to Homma et al[6], both mild and permanent RLS shave been defined as permanent, small, medium, and large by transthoracic echocardiography (TTE) and by Transcranial Doppler (TCD) as previously reported[7].

Model construction and description

The entire domain has been reconstructed using the mean geometrical parameters obtained from the patients imaging data. We modelled blood as a non-Newtonian, incompressible and viscous fluid, with a density of 1060 kg/m3. From a physical point of view, blood was described through the Navier–Stokes[8] and continuity equations, defined as

$$\rho \mathbf{v} \cdot \nabla \mathbf{v} = -\nabla \leq \cdot \tau - \nabla p \quad \text{and} \quad \nabla \cdot \mathbf{v} = 0$$

respectively, where v is the 3D velocity vector, P pressure, r density

and the shear stress term. Moreover, a Carreau model was adopted for describe the viscosity[9]. As per normal anatomy, pulmonary veins were located at the back of the atrium, two on each side at different heights. The in flow domain was defined at the four entrances of the pulmonary veins whereas the mitral valve was considered the outflow domain.Conversely, both crista terminalis and the tricuspid valve were not considered in the analysis, since the aim of the study was to describe the hemodynamic effect on the left side of the heart. All the geometries were reconstructed, segmented and meshed using the open source software Slicer 3D (http://www.slicer.org) and/or Rhinoceros v. 4.0 Evaluation software (McNeel& Associates, Indianapolis, IN). Simulations were conducted using the commercial software ANSYS FLUENT 14.0 (Ansys, Inc., Canonsburg, PA).

Heart chambers geometry and properties

The geometry of the left atrium geometry was compared to a hemi-ellipsoid which had the averaged measures obtained in both long- and short-axis views. At the same manner, also the LAA and the RA were reconstructed. Specifically, the 3D reconstruction of both the RA and LAA were obtained according the method proposed by Hillier et al, using TTE, since a geometrical figure able to represent the chamber is difficult to obtain[10]. Superior vena cava, crista terminalis and tricuspid valve were not reconstructed since primary aim was to assess the rheologic properties of blood across the LAA. The measures of each component of the model have been expressed as the average value ±standard deviation. We adopted the pattern of pulmonary velocities (in cm/s)described by Zhang et al. to simulate the blood flow into the LA, RA and LAA as inflow conditions during sinus heart rhythm[11].

Blood flow in LA and LAA in patients with both mild and permanent RLS was evaluated in terms of vorticity magnitude (1/s). As known, vorticity magnitude represents the magnitude of the vorticity vector while vorticity could be defined as a measure of the rotation of a fluid element as it moves in the domain, defined as the curl of the vector: $\xi = \nabla \times \vec{v}$

A low value of vorticity magnitude could be interpreted as a reduction or even absence of atrial contraction and as consequence, an index of relative blood stagnation[12].

Statistical analysis

Continuous variables were expressed as mean and standard deviation (SD) and compared with Student t-test.All statistical analyses were carried out using SPSS statistical software version 19.0 (SPSS Inc, Chicago, IL, USA). A p value < 0.05 was considered statistically significant.

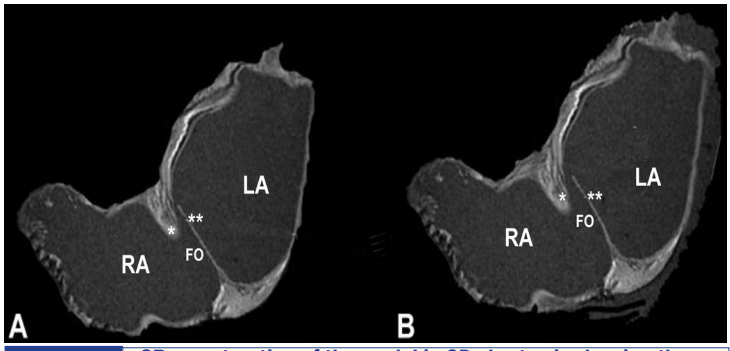

Figure 1: SReconstruction of the model in 2D short axis showing the anatomical relationship between the right atrium (RA), septum primum (*), septum secundum (**), the fossa ovale (FO) and left atrium (LA) in patients with mild (A) and permanent (B) right-to-left shunt (RLS).

Table 1: Echocardiographic measurements used to construct the model. LA: Left atrium; RA: Right Atrium; LAA: Left Atrial appendage.

	All	Mild RLS	Permanent RLS	
0.542 - 1.173	N=65	N=36	N=29	P-value
Pulmonary veins diameter (mm)				
Right-superior	15.5±0.4	15.2±0,.3	15.3±0.1	0.92
Right-inferior	16.3±0.2	16.5±0.2	16.1±0.5	0.93
Left-superior	15.9±0.4	15.7±0.1	16.2±0.3	0.88
Left-inferior	16.8±0.4	16.3±0.3	17.1±0.1	0.94
Mitral valve area (cm2)	4.6±0.8	4.7±0.5	4.6±0.4	0.78
LA area (cm2)	17.7±1.2	17.8±1.0	18.0±0.8	0.75
LA diameter (cm)	3.5±0.6	3.4±0.7	3.6±0.5	0.91
RA minor axis (cm)	3.8±0.9	3.7±1.0	3.9±0.8	0.89
RA major axis (cm)	4.2±0.8	4.1±0.7	4.3±0.7	0.92
LAA				
Length (mm)	27.2±0.4	26.8±0.2	27.4±0.4	0.76
Orifice diameter (mm)	15.4±0.3	15.0±0.2	15.6±0.1	0.80

Results

The anatomical models [Figure 1] and parameters used for model construction and derived from both TTE and cardiac MRI were comparable in permanent versus mild R-L shunting patients [Table 1]. The of the pulmonary veins (PVs) diameters and mitral valve (MV) area in the entire population were 15.5±0.4, 16.3±0.2, 15.9±0.4, 16.8±0.42 mm and 4.6±0.8 mm2, respectively. LAA length and orificediameter were 27.2±0.4 and 15.4±0.3mm, respectively.

To assess the blood flow streamlines in both cases, a cross-sectional area in the short-axis view has been obtained, simulating a different grade of RA-LA shunt.The physiology of the right and left heart's

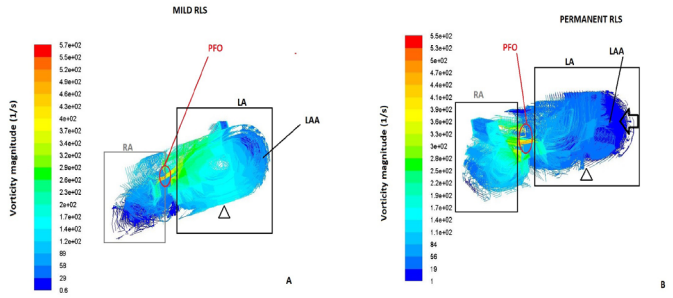

Figure 2: Computational fluid dynamic (CFD) analysis demonstrating a lower vorticity magnitude (1/s) in the left atrium (LA) and left atrial appendage (LAA) (arrow) of patients with permanent RLS (A) compared to those with mild shunting defect (B).

circle was maintained, as demonstrated in both cases; indeed, the right part of the heart appeared with a lower total pressure, according to the physiology of the right circulation, which is characterized by a global lower pressure. Moreover, the total pressure, defined as static + dynamic pressure, showed the presence of a gradient across the PFO. A higher vorticity magnitude was observed in the mild shunt both in the LA (101.12±21.3 vs 88.3±22.6, p=0.02) and LAA (62±14.4 vs32.4±12.3, p<0.01) when compared to the permanent

Table 2: Comparison of vorticity magnitude (1/s) differences between LA and LAA depending on

		LA			LAA	LAA
	Mild RLS	Permanent RLS	p	Mild RLS	Permanent RLS	p <0.01
Vorticity Magnitude (1/s)	101.12±21.3	88.3±22.6	0.02	62±14.4	32.4±12.3	

LA: left atrium; LAA: left atrial appendage; R-L shunting severity.

R-L shunting [Table 2],[Figure 2].

Discussion

Our brief study suggests that the LA vorticities in patients with permanent RLS are different from those with mild/no R-L shunt.A lower vorticity was observed in the case of permanent RLS involving the wall of the LA, especially at the LAA, suggesting a higher stagnation of the blood and reinforcing the hypothesis of a link between PFOand thromboembolic disease as observed in patients with AF.

AF disrupts movement of the leftatrium(LA) and worsensthevitalprognosis by causing thromboembolism.Ultrasound Doppler measurements, phase-contrast magnetic resonance imaging, as well as computational fluid dynamics (CFD) have revealed hemodynamic changes in the LA dueto AF, such as stagnation of blood flow in the LAA[13].

The flow profile in the Left atrial appendage in patients with permanent RLS due to large PFO is very consistent with the one found by both Zhang et al[11] and Koizumi et al[14] in patients with AF. Both studies found atrial wall movement byhigh-frequency fibrillation had a large impact on blood flow stagnation.The relative residence time (RRT),which is an indicator of blood flow stagnation, increased in the upper part of the LAA during AF.

Zhang et al[11] showed that the left atrial appendage is not functional in sinus rhythm because theatrial trans-mitral velocities remained almost identical for atria with and without appendage. However, in atrial fibrillation, a proper atrial contraction is absent, which causes the second emptying velocity (A-wave) tobe missed in both trans-mitral velocity and appendage filling/emptying velocity. Without an adequate blood atrial emptying, vortices generated in the chamber remain high strengths and with longer durations. They induce ineffective emptying of the blood into the atriumand the appendage, which then leads to blood stagnation and subsequent thrombus formation. Our analysis suggests that in presence of severe R-L shunt the vortex movement in the LAA resulted not significant, contributing to the blood flow stasis and resembling the fluid conditions in LAA due to AF.

The contribution of atrial septal aneurysm which per se has been claimed to be involved in LA dysfunction even in the absence of PFO is difficult to assess in the present model, but it is likely to increase the stagnation impairing the LA contraction, conduit, and reservoir functions[15]-[16]. Although to be clinically demonstrated and uniquely speculative, differently from common though, permanent RLS due to PFO might cause the same flow conditions of AF predisposing the LAA and LA to thrombus formation. The traditional hypothesis of Hanley[17], suggested that extremely mobile atrial septal aneurysms are related with atrial fibrillation in adults. Overall, these findings suggest that atrial arrhythmias may be more frequently manifested in patients with atrial septal aneurysms, and that the increased risk of embolism may be due to a higher risk of onset of episodes of paroxysmal atrial fibrillation. An additional hypothesis points to the formation "in loco" of small thrombi capable of becoming lodged in the aneurysmal sac. It might be postulated that in PFO associated-stroke patients the pathogenesis of embolism consists in an in-situs thrombus formation rather than an embolus transiting from right to left chambers.

Study limitation

Our study has several limitations including the intrinsic bias caused by building up a virtual model for the simulation of flow and the lack of the evaluation of the fluid dynamic in a model of AF patients in our population. The former constitutes a limitation but at the same time ensures also stabile homogeneous hemo dynamic conditions which usually are very difficult to obtain in real patients. The latter is due to relative weakness of the software used which allows for a good spatial modelling of cardiac chambers but offers poor calculation of the contribution of rapid myocardial contraction typical of AF.

Conclusion

In conclusion, our CFD study suggests that presence of a severe permanent R-L shunt might cause stagnation in both the LA and LAA simulating the same thrombogenic pathophysiology of atrial fibrillation.

References

1. Rigatelli G, Aggio S, Cardaioli P, Braggion G, Giordan M, Dell'avvocata F, Chinaglia M, Rigatelli G, Roncon L, Chen JP. Left atrial dysfunction in patients with patent foramen ovale and atrial septal aneurysm: an alternative concurrent mechanism for arterial embolism?. JACC Cardiovasc Interv. 2009;2 (7):655–62.
2. Koizumi R, Funamoto K, Hayase T, Kanke Y, Shibata M, Shiraishi Y, Yambe T. Numerical analysis of hemodynamic changes in the left atrium due to atrial fibrillation. J Biomech. 2015;48 (3):472–8.
3. Berthet K, Lavergne T, Cohen A, Guize L, Bousser MG, Le Heuzey JY, Amarenco P. Significant association of atrial vulnerability with atrial septal abnormalities in young patients with ischemic stroke of unknown cause. Stroke. 2000;31 (2):398–403.
4. Jarral OA, Saso S, Vecht JA, Harling L, Rao C, Ahmed K, Gatzoulis MA, MalikIqbal S, Athanasiou T. Does patent foramen ovale closure have an anti-arrhythmic effect? A meta-analysis. Int. J. Cardiol. 2011;153 (1):4–9.
5. Olivares-Reyes A, ChanS, LazarE J, Bandlamud iK, Narla V, Ong K. Atrial septal aneurysm: a new classification in two hundred five adults. J Am Soc Echocardiogr. 1997;10 (6):644–56.
6. Homma S, Sacco RL, Di Tullio MR, Sciacca RR, Mohr J P. Effect of medical treatment in stroke patients with patent foramen ovale: patent foramen ovale in Cryptogenic Stroke Study. Circulation. 2002;105 (22):2625–31.
7. Messé SR, SilvermanI E, Kizer J R, Homma S, Zahn C, Gronseth G, Kasner S E. Practice parameter: recurrent stroke with patent foramen ovale and atrial septal aneurysm: report of the Quality Standards Subcommittee of the American Academy of Neurology. Neurology. 2004;62 (7):1042–50.
8. Cho Y I, Kensey K R. Effects of the non-Newtonian viscosity of blood on flows in a diseased arterial vessel. Part 1: Steady flows. Biorheology. 1991;28 (3-4):241–62.
9. Johnston BM, Johnston PR, Corney St, Kilpatrick D. Non-Newtonian blood flow in human right coronary arteries: steady state simulations. J Biomech. 2004;37

(5):709–20.

10. Hillier D, Czeilinger Z, Vobornik A, Rekeczky C. Online 3-D reconstruction of the right atrium from echocardiography data via a topographic cellular contour extraction algorithm. IEEE Trans Biomed Eng. 2010;57 (2):384–96.
11. Zhang LT, Gay M. Characterizing left atrial appendage functions in sinus rhythm and atrial fibrillation using computational models. J Biomech. 2008;41 (11):2515–23.
12. Cibis M, Lindahl T L, Ebbers T, Karlsson LO, Carlhäll CJ. Left Atrial 4D Blood Flow Dynamics and Hemostasis following Electrical Cardioversion of Atrial Fibrillation. Front Physiol. 2017;8.
13. Delgado V, Di Biase L, Leung M, Romero J, Tops LF, Casadei B, Marrouche N, Bax JJ. Structure and Function of the Left Atrium and Left Atrial Appendage: AF and Stroke Implications. J. Am. Coll. Cardiol. 2017;70 (25):3157–3172.
14. Demir M, Ozmen G, Keçoğlu S, Günay T, Melek M. Right and left atrial appendage function in patients with atrial septal aneurysm without patent foramen ovale. Acta Cardiol. 2012;67 (4):457–60.
15. Rigatelli G, Ronco F Cardaioli P, Dell'avvocata F, Braggion G, Giordan M, Aggio S. Incomplete aneurysm coverage after patent foramen ovale closure in patients with huge atrial septal aneurysm: effects on left atrial functional remodeling. J Interv Cardiol. 2010;23 (4):362–7.
16. Goch A, Banach M, Piotrowski G, Szadkowska I, Goch J H. Echocardiographic evaluation of the left atrium and left atrial appendage function in patients with atrial septum aneurysm: implications for thromboembolic complications. Thorac Cardiovasc Surg. 2007;55 (6):365–70.
17. Hanley P C, Tajik A J, Hynes J K, Edwards W D, Reeder G S, Hagler D J, Seward J B. Diagnosis and classification of atrial septal aneurysm by two-dimensional echocardiography: report of 80 consecutive cases. J. Am. Coll. Cardiol. 1985;6 (6):1370–82.